IECC 2018

sciforum

Conference Proceedings Paper

2D supramolecular Structure for a Chiral Heterotrinuclear $Zn^{II}_2Ho^{III}$ Complex through Varied H-bonds Connecting Solvates and Counterions

Julio Corredoira, Matilde Fondo, Jesús Sanmartín-Matalobos and Ana M. García-Deibe *

Dpt. of Inorganic Chemistry. Faculty of Chemistry. Campus Vida. Universidade de Santiago de Compostela. Santiago de Compostela. 15782 SPAIN. julio_corredoira@hotmail.com; matilde.fondo@usc.es (J.C.); jesus.sanmartin@usc.es; ana.garcia.deibe@usc.es (J.S.-M.)

* Correspondence: ana.garcia.deibe@usc.es; Tel.: +34-981814237

Abstract: We report the crystal structure of $[Zn^{II}_2Ho^{III}(L)(ald)(HO)(H_2O)_3(MeCN)](NO_3)_2{\cdot}EtOH$ [being H_3L = 2-(5-bromo-2-hydroxy-3-methoxyphenyl)-1,3-bis[4-(5-bromo-2-hydroxy-3-methoxy phenyl)-3-azabut-3-enyl]-1,3-imidazolidine) and Hald = 5-bromo-2-hydroxy-3-methoxy-benzaldehyde]. Despite the presence of two bulky multidentate ligands, as well as several monodentate ligands surrounding the nonacoordinate holmium cation, and the two pseudooctahedral zinc ions, the intricate H-bonded system formed by this chiral heterotrinuclear complex is only expanded in a 2D supramolecular structure. The interactions involve the nitrate counterions and the solvated ethanol, in such way that each complex unit is connected to an identical enantiomer, and to two units of inverted chirality through H bonds.

Keywords: H-bond system; metallosupramolecular structure; heterotrinuclear complex; holmium

1. Introduction

Coordination chemistry of lanthanoids has experimented a substantial development in past years. The interest in this area is closely related to that in single-molecule magnets (SMMs) and single-ion magnets (SIMs), and their potential applications [1]. Concurrently, a particular interest has been devoted to heteronuclear {*s*-/3*d*-4*f*}-coordination complexes, as their combination can afford different properties, and hence, new polyfunctional molecules could arise [2–5]. For instance, the combination of zinc ions, and changes in the ancillary ligands could influence not only the anisotropy barrier [6], but it can additionally afford luminescent properties [6–10]. In this sense, we are particularly interested in obtaining lightluminescent molecular magnets. Thus, we have been recently involved in a research programme aiming to prepare, characterise and study not only discrete pure lanthanoid (Dy, Er, Tb) complexes, but also hybrid Zn-Ln polynuclear complexes containing one of the two polytopic ligands shown in Scheme 1 [11,12].

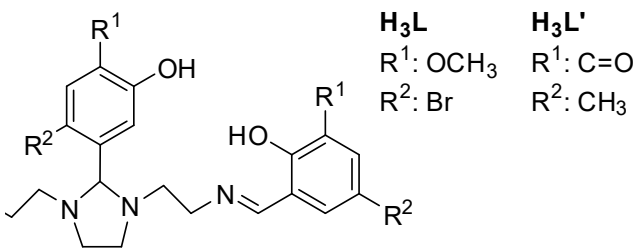

Scheme 1. Ligands used in our work. In this particular case we have employed H_3L.

As a result of this previous work, we have found that complexes as {[ZnDy(HL)(NO_3)(OAc)(CH_3OH)](NO_3)}·1.25CH_3OH·0.25H_2O; [Zn_2Dy(L)(NO_3)$_2$(OAc)$_2$(H_2O)] and [Zn_2Er(L)(NO_3)$_2$(OAc)$_2$(H_2O)]·1.5H_2O behave as induced SIMs [11], while [Zn_2Dy(L')(NO_3)$_3$(OH)] behaves as a fluorescent SIM [12].

As an extension of this work, in this occasion we have tried to combine zinc(II) and holmium(III) ions with H_3L (Scheme1), with the aim of getting further insight into the features of new Zn−Ho systems. The reason of this choice is a not so usual use of holmium for preparing this type of materials, if compared with dysprosium, or even with erbium, but also providing interesting results at a magnetic level [1,5,13,14].

2. Experimental

2.1. Materials and Methods

All chemical reagents were purchased from commercial sources and used as received without further purification.

2.2. Synthesis of [$Zn^{II}_2Ho^{III}$(L)(ald)(HO)(H_2O)(MeCN)](NO_3)$_2$·EtOH

The ligand used in this work, 2-(5-bromo-2-hydroxy-3-methoxyphenyl)-1,3-bis[4-(5-bromo-2-hydroxy-3-methoxy phenyl)-3-azabut-3-enyl]-1,3-imidazolidine) (H_3L, Scheme 1), was obtained as described in literature [11]. This three-armed ligand was subsequently employed to prepare the homodinuclear zinc(II) complex [Zn_2(L)(OAc)], by using a method that has been also previously described by us [11]. With the aim of obtaining a heterotrinuclear complex, a methanol solution (8 mL) of Ho(NO_3)$_3$·5H_2O (0.104 g, 0.24 mmol) was added to a suspension of [Zn_2(L)(OAc)] (0.23 g, 0.24 mmol) in CH_3CN (16 mL). This mixture was stirred at room temperature for ca. 15 hours, giving rise to a yellow solution. The volume of this solution was firstly reduced to 10 mL in a rotary evaporator, and then, the solution was slowly evaporated at room temperature, but without yielding crystals. Hence, the yellow powdery precipitate was tried to recrystallise in different conditions. The best results were obtained from a 2:1 acetonitrile:ethanol mixture, after a very slow evaporation. This latter solution allowed the formation of small yellow single crystals, which were suitable for X-ray diffraction studies. Data collected correspond to [Zn_2Ho^{III}(L)(ald)(HO)(H_2O)(MeCN)](NO_3)$_2$·EtOH (being Hald = 5-bromo-2-hydroxy-3-methoxybenzaldehyde). As the amount isolated was very scarce, and given that it resulted to be by-product, no further characterisation was performed.

2.3. Crystal Structure Determination

Single crystals of [Zn_2Ho^{III}(L)(ald)(HO)(H_2O)(MeCN)](NO_3)$_2$·EtOH were obtained as detailed above. Data were collected at 100 K on a Bruker Kappa APEXII CCD diffractometer employing graphite monochromated Mo-Kα (λ = 0.71073 Å) radiation. Multi-scan absorption corrections were applied using SADABS [15].

The structure was solved by standard direct methods, employing SHELXT [16], and then it was refined by full-matrix leastsquares techniques on F^2, using SHELXL [17]. All non-hydrogen atoms, including counterions and solvates, were anisotropically refined. Hydrogen atoms were included in the structure factor calculations in geometrically idealised positions in most of cases. Hydrogen atoms potentially involved in classic H bonds were located in Fourier maps, and then they were refined with thermal factors depending on the parent atoms.

Crystal data and experimental parameters relevant to the structure determinations are listed in Table 1. Supplementary crystallographic data for this paper have been deposited at Cambridge Crystallographic Data Centre (CCDC-1843238) can be obtained free of charge via www.ccdc.cam.ac.uk/conts/retrieving.html.

Table 1. X-ray crystallographic data for $[Zn_2Ho^{III}(L)(ald)(HO)(H_2O)(MeCN)](NO_3)_2{\cdot}EtOH$.

Formula	$C_{40}H_{46}Br4HoN_5O_{13}Zn_2{\cdot}2(NO_3){\cdot}C_2H_6O$
M_r	1590.21
Crystal dimensions (mm)	0.18 × 0.12 × 0.04
Crystal System, Space group	Monoclinic, $P2_1/n$
a, b, c (Å)	12.930 (1), 17.7500 (12), 17.7500 (12)
α, β, γ (°)	90, 101.885(5), 90
θ Ranges (°)	2.0 – 28.3
V(Å^3), μ/ mm^{-1}	5383.1 (7), 5.39
Z	4
F(000)	3120
D_x/ g·cm^{-3}	1.962
−h, h/−k, k/−l, l	−17, 17 / −23, 23 / −31, 31
Total, unique and [$I > 2\sigma(I)$] reflections	180748, 13340, 10903
No. of reflections, restraints, parameters	13340, 0, 692
R_{int}	0.082
Final R, wR	0.056, 0.119
R, wR (all data)	0.074, 0.126
$\Delta\rho_{max}$, $\Delta\rho_{min}$ (e/Å^3)	2.26, −3.39

3. Results and Discussion

3.1. Synthetic Method

Keeping in mind the magnetic results previously obtained with H_3L and H_3L', our goal was obtaining heterotrinuclear holmium(III) and zinc(II) complexes with H_3L. The synthetic method was designed on the base of our previous experience with H_3L [11], and H_3L' [12] (Scheme 1). A template method using appropriate molar ratios of the corresponding aldehyde, tetraamine and metal salts had resulted useful to obtain mononuclear and even heteronuclear complexes with H_3L' (Scheme 1) [12], but this method was not suitable for H_3L, as the previous isolation of the tricondensed ligand was necessary to prepare its complexes.

By direct reaction of H_3L with dysprosium(III), erbium(III) and terbium(III) nitrates and zinc acetate $[Zn^{II}Ln^{III}(HL)(NO_3)(OAc)(CH_3OH)](NO_3)$ could be obtained, even using 1:1 or 1:2 molar ratios of the metal salts [11]. We had to employ the homodinuclear metalloligand $[Zn_2(L)(OAc)]$ as starting material to prepare complexes of the $[Zn_2Ln(L)(NO_3)_2(OAc)_2(H_2O)]$ type (Ln = Dy^{III}, Er^{III}). By contrast, this method also failed when using Tb^{III}, as it also produces a heterodinuclear complex [11].

Unfortunately, and despite multiple attempts made with different methods, no pure samples of di- or triheteronuclear analogous with holmium(III) ions could be isolated. In fact, the only pure and crystalline compound that has been accurately identified was a by-product identified as $[Zn^{II}_2Ho^{III}(L^3)(ald)(HO)(H_2O)(MeCN)](NO_3)_2{\cdot}EtOH$ by its crystal structure (Figure 1). It is clear that both the deprotonated aldehyde ligand (ald^-), and the hydroxide ion appear resulting from some hydrolysis occurred during either the reaction, or the recrystallisation processes.

Despite the high stability shown by this type of three-armed ligands when we had worked with them [11,12 and own references therein], the reason of these fruitless results could be related to reaction or/and crystallisation periods longer than usual, with a partial decomposition of H_3L. This fact had been previously detected for another related ligand [18]. Unfortunately, the lack of an enough amount of sample, with a guaranteed purity, has avoided to perform further studies of this complex.

3.2. Spatial Arrangement of $[Zn^{II}_2Ho^{III}(L^3)(ald)(HO)(H_2O)(MeCN)]^{2+}$

Despite the symmetry of the three-armed H_3L ligand (Scheme 1), and even of both Zn···Ho distances, $[Zn^{II}_2Ho^{III}(L)(ald)(HO)(H_2O)(MeCN)]^{2+}$ is chiral. In Figure 1, we can see that enantiomer where the chiral C12, N2 and N3 atoms are displaying *S* configurations. The main geometric parameters are listed in Table 2.

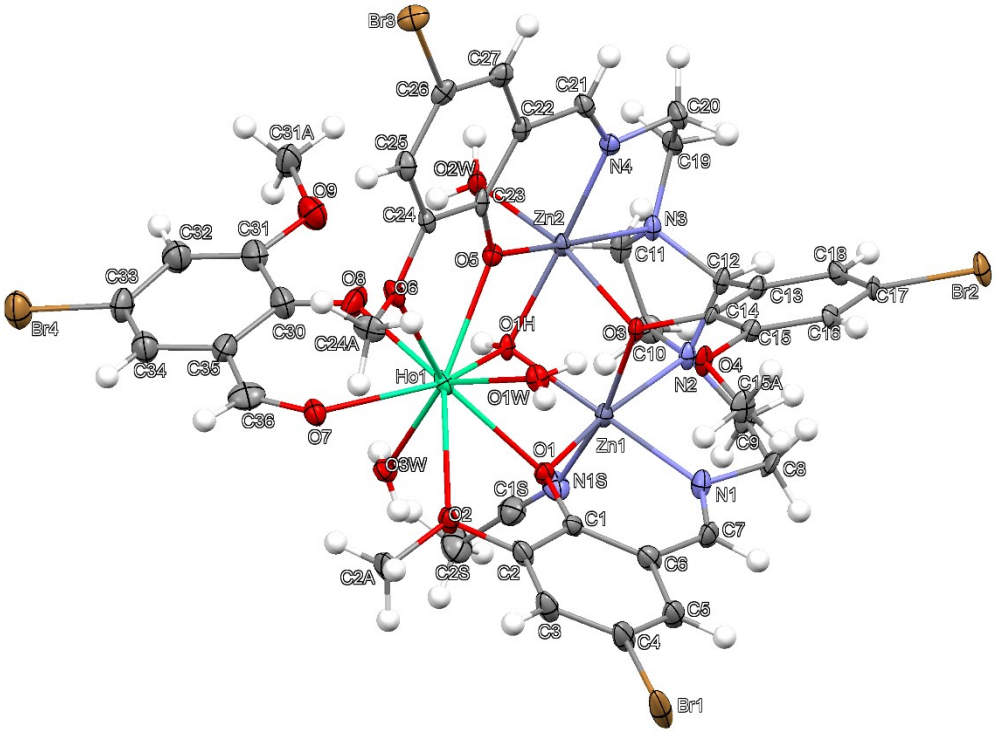

Figure 1. Ellipsoid view of the (*S;S;S*) enantiomer of $[Zn^{II}_2Ho^{III}(L)(ald)(HO)(H_2O)(MeCN)]^{2+}$.

Table 2. Main geometric parameters for $[Zn_2Ho^{III}(L)(ald)(HO)(H_2O)(MeCN)](NO_3)_2{\cdot}EtOH$.

Zn1-O1H	2.018(4)	Zn2-O1H	2.031(4)	Ho1-O8	2.315(5)
Zn1-N1	2.055(6)	Zn2-N4	2.048(5)	Ho1-O5	2.328(4)
Zn1-O1	2.056(4)	Zn2-O5	2.054(4)	Ho1-O1H	2.348(4)
Zn1-O3	2.122(4)	Zn2-O3	2.124(4)	Ho1-O1	2.371(4)
Zn1-N1S	2.203(6)	Zn2-O2W	2.132(5)	Ho1-O3W	2.380(4)
Zn1-N2	2.250(5)	Zn2-N3	2.201(5)	Ho1-O7	2.387(5)
O1H-Zn1-N1	169.0(2)	O1H-Zn2-N4	170.68(19)	Ho1-O1W	2.423(4)
O3-Zn1-N1S	168.5(2)	O3-Zn2-O2W	166.70(18)	Ho1-O6	2.660(5)
O1-Zn1-N2	170.48(18)	O5-Zn2-N3	169.80(19)	Ho1-O2	2.671(5)
O8-Ho1-O5	73.77(18)	O1H-Ho1-O1	68.75(15)	O1-Ho1-O3W	74.89(15)
O8-Ho1-O1H	75.42(19)	O8-Ho1-O3W	77.42(18)	O8-Ho1-O7	71.27(19)
O5-Ho1-O1H	69.58(15)	O1H-Ho1-O3W	78.31(15)	O3W-Ho1-O7	72.50(16)
O5-Ho1-O1W	72.03(15)	O1-Ho1-O1W	73.56(15)	O8-Ho1-O6	79.79(18)

Chirality is related not only to the irregular coordination environment of the holmium atom, but also to the two different solvent molecules (MeCN and water) coordinated to each internal zinc atom. These zinc ions show distorted octahedral environments, which are sharing one of their faces with the pseudo-polyhedron around Ho1 (Figure 2), in contrast with the pentacoordinate $[Zn_2(L)(OAc)]$ precursor. This change is favoured by the substitution of the μ_2-η^1:η^1 bridging acetate by a tiny μ_3-OH anion. This also leads to a significative folding of both *N,O,O,N* donor sites to ca. 73.4° (only ca. 26.3°

in [Zn_2(L)(OAc)]), and the subsequent coordination of these two solvates on those apexes opposite to the phenoxy group (O3) attached to the central bridging arm of L^{3-}.

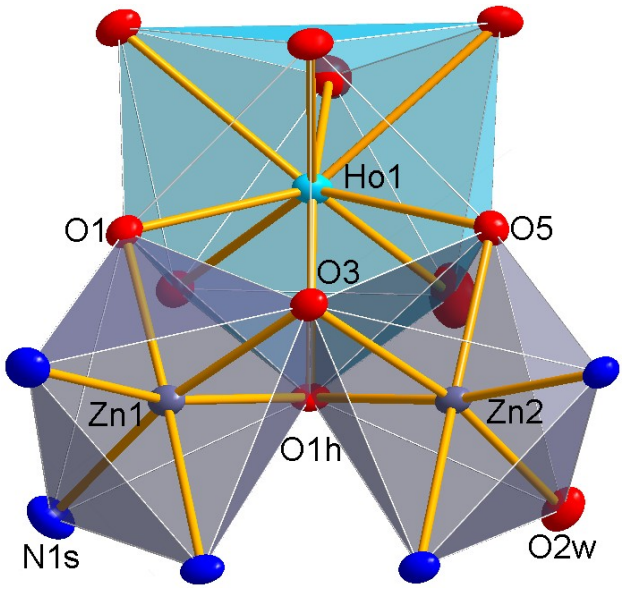

Figure 2. Pseudo-polyhedra of the coordination environments of the holmium(III) and zinc(II) ions for the (*S,S,S*) enantiomer of $[Zn^{II}_2Ho^{III}(L)(ald)(HO)(H_2O)(MeCN)]^{2+}$.

With regard to the holmium(III) ion, it is surrounded by nine O atoms that belong to the phenoxy and methoxy groups attached to the two terminal arms of L^{3-} (O1, O2, O5, O6) and to the deprotonated aldehyde residue (O7, O8), as well as to the hydroxide ion (O1h), and to two water molecules (O1w, O3w). The degree of distortion of this HoO_9 coordination sphere with respect to an ideal nine-vertex polyhedron was calculated with the SHAPE software [19], and it indicates that nearly corresponds to a "muffin-like" geometry (Figure 2).

Curiously, this complex noticeably reminds to $[Zn_2Dy(L')(NO_3)_3(OH)]$ [12], more than to those ones derived from L^{3-} and [Zn_2(L)(OAc)] [11]. Thus, as occurring in $[Zn_2Dy(L')(NO_3)_3(OH)]$, the tight μ_3-η^1:η^1:η^1-HO^- bridge leads to the three metal ions to appear as an isosceles triangle, since d(Zn1···Zn2), is *ca.* 3.04, while both Zn···Ho1 distances are about 3.45 Å. These intermetallic distances are similar to those found for other Zn-Ho complexes with polycompartmental Schiff bases [20,21], and also with the 3-EtO-salen^{2-} ligand [22,23]. By contrast, the Zn···Ln distances are clearly asymmetric in $[Zn_2Ln(L)(OAc)_2(NO_3)_2(H_2O)]$ (Ln = Dy^{III} and Er^{III}) (about 3.45 and 4.7 Å) [11].

3.3. Packing Scheme for $[Zn_2Ho^{III}(L)(ald)(HO)(H_2O)(MeCN)](NO_3)_2{\cdot}EtOH$

With the presence of so many O and N atoms in the ligands, three coordinated water molecules, an ethanol solvate, and two nitrate counterions is not surprising that this complex can give rise to an intricate H bonding scheme. However, this packing scheme presents some interesting features at a supramolecular level. To simplify its study, only classic O-H···O bonds are listed in Table 2, but several bifurcations, and many C-H···A interactions (A = O or Br) have been also detected. The basic O-H···O network is shown in Figure 3.

It is evident that both the enveloping three-armed ligand and the ancillary aldehyde ligand can exert a considerable steric hindrance for the intermolecular propagation of classic H bonds. Nevertheless, this does not avoid the multidirectional expansion of multiple O-H···O bonds from the three water molecules and the hydroxide anion to form an extended supramolecular structure. Curiously, this growth exclusively occurs in a perfect 2D-arrangement, parallel to the *b* axis of the unit cell (Figures 3 and 4).

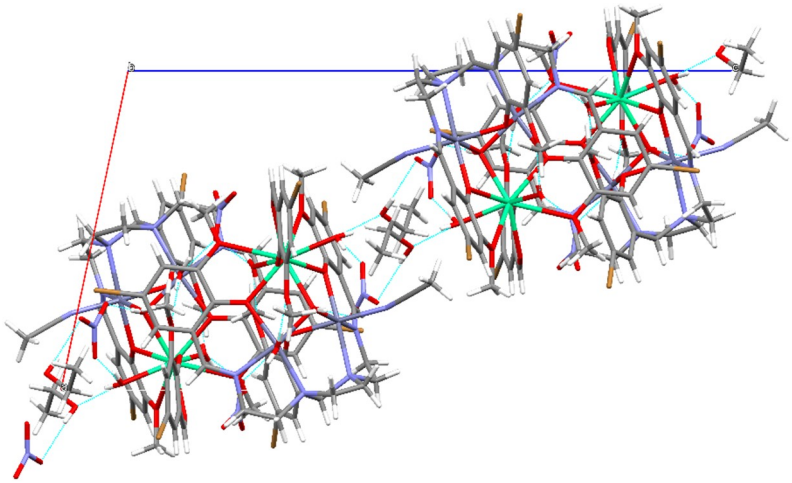

Figure 3. Sticks representation of one of the 2D-layers connected through classic O-H··O bonds (blue and red dotted lines) formed by $[Zn_2Ho^{III}(L)(ald)(HO)(H_2O)(MeCN)](NO_3)_2{\cdot}EtOH$.

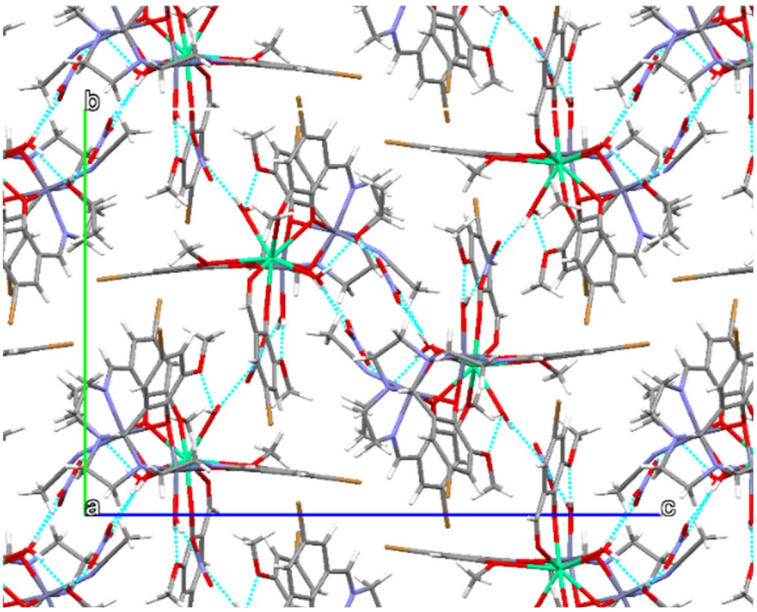

Figure 4. Sticks view perpendicular to the *a* face of the monoclinic unit cell showing the classic O-H···O interactions (blue and red dotted lines).

Table 2. Main classic H bonds found for $[Zn_2Ho^{III}(L)(ald)(HO)(H_2O)(MeCN)](NO_3)_2{\cdot}EtOH$.

D-H···A	d(D-H)	d(H...A)	d(D...A)	<(DHA)
O(1H)-H(1H)···O(22)	0.87	1.90	2.769(6)	177.6
O(1W)-H(1W1)···O(3)	0.80	2.35	3.069(6)	149.9
O(1W)-H(1W1)···O(4)	0.80	2.20	2.848(6)	137.7
O(1W)-H(1W2)···O(10)	0.83	2.09	2.888(8)	161.3
O(2W)-H(2W1)···O(9)	0.74	2.16	2.877(7)	164.2
O(2W)-H(2W2)···O(10)$^{\#1}$	0.84	2.00	2.816(8)	162.9
O(3W)-H(3W1)···O(1S)	0.73	1.98	2.694(7)	164.1
O(3W)-H(3W2)···O(21)	0.78	2.05	2.807(7)	164.7
O(1S)-H(1S)···O(23)$^{\#2}$	0.84	1.96	2.778(8)	163.0

$^{\#1}$ −x+3/2,y−1/2,−z+1/2; $^{\#2}$ −x+2,−y,−z.

To form these supramolecular layers, each heterotrinuclear cation is simultaneously acting as H-donor, through the μ_3-HO group and a water molecule coordinated to the holmium atom, connected to two O acceptors belonging to one of the nitrate counterions, while the water molecule is also linked to a solvated ethanol molecule. This substructure is mutually connected to an inverted one, as the third O atom of each nitrate is acting as an H-acceptor for the ethanol solvate of the other substructure. Additionally, a second water molecule coordinated to the holmium atom displays an intramolecular H-bond to the methoxy group of the central arm of L^{3-}, and an intermolecular one involving a second nitrate counterion.

Finally, the water molecule coordinated to one of the zinc atoms participates in an intramolecular bifurcated H-bond with the deprotonated aldehyde ligand, while it is additionally connected to an O atom of a third nitrate anion, which also participate in the second type of interactions described above. Thus, each one of the enantiomers of the complex is H-bonded to three nitrate ions, and it is also connected to an identical enantiomer, and to two units of inverted chirality, but all of them extended on infinite 2D sheets. These interactions are illustrated by Figures 3 and 4.

The surface of each layer so formed presents hydrophobic character, as the predominant bonds are mostly C-H, corresponding to imidazolidine rings, ethylene chains and aromatic rings. Likewise, C-Br bonds and some nitrate counterions scarcely accessible are forming part of this surface (Figure 3). Consequently, these layers are not connected via classic bonds, but through C-H···A bonds (A = O or Br). This behaviour had been previously observed for other related ligands [24].

4. Conclusions

The heterotrinuclear complex $[Zn_2Ho^{III}(L)(ald)(HO)(H_2O)(MeCN)](NO_3)_2{\cdot}EtOH$ is chiral due to the asymmetry of the different coordination environments. Despite the presence of multiple and varied potential donors and acceptors for H bonding, the packing scheme is basically bidimensional, and mostly based on classic O-H···O bonds. The surface of the layers formed is rather hydrophobic, and the interaction between layers mostly depends on C-H···Br and C-H···O interactions.

Supplementary Materials: Supplementary crystallographic data for this paper have been deposited at Cambridge Crystallographic Data Centre (CCDC-1843238) can be obtained free of charge via www.ccdc.cam.ac.uk/conts/retrieving.html.

Acknowledgments: Financial support from Ministerio de Economía y Competitividad (MINECO, CTQ2014-56312-P) is gratefully acknowledged.

Author Contributions: The manuscript was written through contributions of all authors. All authors have given approval to the final version of the manuscript.

References

1. Woodruff, D.N.; Winpenny, R.E.P.; Layfield, R.A. Lanthanide single-molecule magnets. *Chem. Rev*. **2013**, *113*, 5110–5148.
2. Osa, S.; Kido, T.; Matsumoto, V.Re.N.; Pochaba, A.; Mrozinski, J. A Tetranuclear 3d−4f Single Molecule Magnet: $[Cu^{II}LTb^{III}(hfac)_2]_2$. *J. Am. Chem. Soc.* **2004**, *126*, 420–421.
3. Papatriantafyllopoulou, C.; Wernsdorfer, W.; Abboud, K.A.; Christou, G. $Mn_{21}Dy$ Cluster with a Record Magnetization Reversal Barrier for a Mixed 3*d*/4*f* Single-Molecule Magnet. *Inorg. Chem*. **2011**, *50*, 421–423.
4. Moreno Pineda, E.; Chilton, N.F.;Tuna, F.; Winpenny, R.E.P.; McInnes, E.J.L. Systematic Study of a Family of Butterfly-Like $\{M_2Ln_2\}$ Molecular Magnets (M = Mg^{II}, Mn^{III}, Co^{II}, Ni^{II}, and Cu^{II}; Ln = Y^{III}, Gd^{III}, Tb^{III}, Dy^{III}, Ho^{III}, and Er^{III}). *Inorg. Chem*. **2015**, *54*, 5930–5941.
5. Biswas, S.; Bag, P.; Das, S.; Kundu, S.; van Leusen, J.; Kögerler, P.; Chandrasekhar, V. Heterometallic $[Cu_2Ln_3]$ (Ln = Dy^{III}, Gd^{III} and Ho^{III}) and $[Cu_4Ln_2]$ (Ln = Dy^{III} and Ho^{III}) Compounds: Synthesis, Structure, and Magnetism. *Eur. J. Inorg. Chem*. **2017**, 1129–1142.

6. Costes, J.P.; Titos-Padilla, S.; Oyarzabal, I.; Gupta, T.; Duhayon, C.; Rajaraman, G.; Colacio, E. Effect of ligand substitution around the Dy^{III} on the SMM properties of dual-luminescent Zn−Dy and Zn−Dy−Zncomplexes with large anisotropy energy barriers: a combined theoretical and experimental magnetostructural study. *Inorg. Chem*. **2016**, *55*, 4428−4440.
7. Yue, S.-T.; Wei, Z.-Q.; Wang, N.; Liu, W.-J.; Zhao, X.; Chang, L.-M.; Liu, Y.-L.; Mo, H.-H.; Cai Y.-P. Three novel microporous 3D heterometallic 3d–4f coordination polymers: Synthesis, crystal structures and photoluminescence properties. *Inorg. Chem. Commun*. **2011**, *14*, 1396–1399.
8. Das, S.; Bejoymohandas, K.S.; Dey, A.; Biswas, S.; Reddy, M.L.P.; Morales, R.; Ruiz, E.; Titos-Padilla, S.;. Colacio, E; Chandrasekhar, V. Amending the Anisotropy Barrier and Luminescence Behavior of Heterometallic Trinuclear Linear [$M^{II}Ln^{III}M^{II}$] (Ln^{III}=Gd, Tb, Dy; M^{II}=Mg/Zn) Complexes by Change from Divalent Paramagnetic to Diamagnetic Metal Ions. *Chem.–Eur. J*. **2015**, *21*, 6449–6464.
9. Meng, Y.-S.; Jiang, S.-D.; Wang, B.-W.; Gao S. Understanding the Magnetic Anisotropy toward Single-Ion Magnets. *Acc. Chem. Res*. **2016**, *49*, 2381−2389.
10. Wang, Y.-M.; Wang, Y.; Wang, R.-X.; Qiu, J.-Q.; Chi, Y.-X.; Jin, J.; Niu, S.-Y. Syntheses, structures and photophysical properties of a series of Zn-Ln complexes. *J. Phys. Chem. Solids*, **2017**, *104*, 221–227.
11. Fondo, M.; Corredoira-Vázquez, J.; García-Deibe, A.M.; Sanmartín-Matalobos, J.; Herrera, J.M.; Colacio E. Designing Ligands to Isolate ZnLn and Zn2Ln Complexes: Field-Induced Single-Ion Magnet Behavior of the ZnDy, Zn_2Dy, and Zn_2Er. *Inorg. Chem.* **2017**, *56*, 5646−5656.
12. Fondo, M.; Corredoira-Vázquez, J.; Herrera-Lanzós, A.; García-Deibe, A.M.; Sanmartín-Matalobos, J.; Herrera, J.M.; Colacio, E.; Nuñez, C. Improving the SMM and luminescence properties of lanthanide complexes with LnO9 cores in the presence of ZnII: an emissive Zn2Dy single ion magnet. *Dalton Trans.* **2017**, *46*, 17000–17009.
13. Bag, P.; Chakraborty, A.; Rogez, G.; Chandrasekhar, V. Pentanuclear Heterometallic {$Mn^{III}_2Ln_3$} (Ln = Gd, Dy, Tb, Ho) Assemblies in an Open-Book Type Structural Topology: Appearance of Slow Relaxation of Magnetization in the Dy(III) and Ho(III) Analogues. *Inorg. Chem*. **2014**, *53*, 6524–6533.
14. Vignesh, K.R.; Langley, S.K.; Murray, K.S.; Rajaraman, G. Exploring the Influence of Diamagnetic Ions on the Mechanism of Magnetization Relaxation in {$Co^{III}_2Ln^{III}_2$} (Ln = Dy, Tb, Ho) "Butterfly" Complexes. *Inorg. Chem*. **2017**, *56*, 2518–2532.
15. SADABS, Area-Detector Absorption Correction; Siemens Industrial Automation, Inc.: Madison, WI, USA, 1996.
16. Sheldrick, G.M. SHELXT–Integrated space-group and crystal-structure determination. *Act*a *Cryst*. **2015**, *A71*, 3–8.
17. Sheldrick, G.M. Crystal structure refinement with SHELXL. *Acta Cryst.* **2015**, *C71*, 3–8.
18. Fondo, M.; Ocampo, N.; García-Deibe, A.M.; Ruiz, E.; Tercero, J.; Sanmartín, J. Discovering the complex Chemistry of a simple Ni^{II}/H_3L system: Magnetostructural characterization and DFT calculations of di- and polynuclear nickel(II) compounds. *Inorg. Chem*. **2009**, *48*, 9861–9873.
19. Llunell, M.; Casanova, D.; Cirera, J.; Alemany, P.; Alvarez, S. SHAPE: Program for the stereochemical analysis of molecular fragments by means of continuous shape measures and associated tools. University of Barcelona: Barcelona, Spain, 2010.
20. Akine, S.; Taniguchi, T.; Nabeshima, T. Helical Metallohost-Guest Complexes via Site-Selective Transmetalation of Homotrinuclear Complexes. *J. Am. Chem. Soc*. **2006**, *128*, 15765–15774.
21. Amjad, A.; Madalan, A.M.; Andruh, M.; Caneschi, A.; Sorace, L. Slow relaxation of magnetization in an isostructural series of zinc–lanthanide complexes: An integrated EPR and AC susceptibility study. *Chem. Eur. J*. **2016**, *22*, 12849–12858.
22. Maeda, M.; Hino, S.; Yamashita, K.; Kataoka, Y.; Nakano, M.; Yamamurac, T.; Kajiwara, T. Correlation between slow magnetic relaxation and the coordination structures of a family of linear trinuclear Zn(II)–Ln(III)–Zn(II) complexes (Ln = Tb, Dy, Ho, Er, Tm and Yb). *Dalton Trans*. **2012**, *41*, 13640–13648.
23. Wong, W.-K. Liang, H.; Wong, W.-Y.; Cai, Z.; Lib, K.-F.; Cheah, K.-W. Synthesis and near-infrared luminescence of 3d-4f bi-metallic Schiff base complexes. *New J. Chem*. **2002**, *26*, 275–278.

24. García-Deibe, A.M.; Fondo, M.; Corredoira-Vázquez, J.; Fallah, M.S.E.; Sanmartín-Matalobos, J. Hierarchical *assembly* of antiparallel homochiral sheets formed by hydrogen-bonded helixes of a trapped-valence Co^{II}/Co^{III} complex. *Cryst. Growth Des*. **2017**, *17*, 467–473.